UPDATES ON HARDWARE DEVELOPMENTS FOR SPring-8-II

T. Watanabe[†], S. Takano, JASRI/RSC, 679-5148 Hyogo, Japan
H. Tanaka, RIKEN SPring-8 Center (RSC), 679-5198 Hyogo, Japan
on behalf of SPring-8-II Upgrade Working Group

Abstract

A major upgrade of SPring-8, SPring-8-II, targeting substantial improvements in the light source performance has been designed based on a five-bend achromat lattice at an electron energy of 6 GeV [1, 2], and hardware developments have been extensively implemented. After the several year developments, a test half-cell has been constructed in 2018 to investigate the feasibility of each component as well as whole assemblies. In the paper, we present overall status of hardware developments, including the test half-cell construction.

INTRODUCTION

The third generation synchrotron radiation facility SPring-8 has commenced user operations in 1997, and the new generation light source based on X-ray Free Electron Laser, SACLA, started in 2011. The combination of the two side-by-side large light sources gives unique capabilities for cutting edge sciences and other applications. The role is expected to become larger and larger.

Currently, the SPring-8 accelerator complex is composed of a 1 GeV linac, an 8 GeV booster synchrotron, and an 8 GeV storage ring with insertion devices. SACLA consists of an 8 GeV linac and a series of in-vacuum undulators. Between the SACLA linac and the storage ring, a new beam transport, named XSBT, has been constructed so that we can share the SACLA linac as a high quality beam injector for both of the two light sources. Bunch-by-bunch on-demand injection from SACLA to the storage ring is being prepared, and it is planned to start prior to the major upgrade.

For SPring-8-II, we plan to replace most of storage ring components. Obviously, the brilliance and coherence of light are one of figure of merits for light sources. We also regard the stability and reliability as important, because these features are strengths of ring-based light source. Another underlying concept for SPring-8-II is the energy saving. We aim to achieve the significant leap of the light source performance with *less* power consumption. Further, we assume it mandatory to shut down the light source no longer than about a year.

With these concepts in mind, we have designed a five-bend lattice at an electron energy of 6 GeV. The resulting emittance is estimated to be 100 pm•rad with undulator damping, which is expected to provide tens of higher brilliance compared with current SPring-8. The decrease of the electron energy will be compensated by shorter period undulators for providing the same spectral range of undulator radiation. Key developments are permanent magnet based dipole magnets, small diameter multipole magnets, precise alignment schemes, narrow aperture stainless steel vacuum chambers, and accurate beam position monitors, etc. The beam injection is also one of key issues, but in the paper we shall not discuss it due to the limitation of pages.

MAGNETS

Dipole and Multipole Magnets

Permanent magnets consume no energy, and there is no risk of power supply or water system failure [3, 4]. At SPring-8, the feasibility study of permanent magnet for future accelerators had been initiated prior to the upgrade project, then after several year proof-of-principle studies, we started the developments for SPring-8-II. It is now assumed that all the five bending magnets, i.e., four longitudinal gradient bending magnets (LGBs) and one normal bending magnet, will be permanent magnet based [4].

Figure 1 shows a picture of the fabricated LGB for SPring-8-II (TOKIN Co. Ltd.). It consists of three segments, each of which generates a dipole field of 0.54, 0.27, and 0.19 T, respectively. The gap is same at 25 mm for all the segments for minimizing fringe and other undesirable fields [4]. The field quality is significantly improved by high permeability iron yokes between permanent magnet and electron beam. The temperature coefficient of permanent magnet is compensated by using Fe-Ni alloy. Demagnetization is expected to be small because Sm_2Co_{17} magnet is selected. The magnet is equipped with mechanically moving iron plates ("inner plates") that enables us to adjust the dipole fields in a smooth way. NMR tesla meter heads are also attached in the back yoke so drifts of magnetic fields can be observed with adequate resolution and reliability for years. Figure 2 is an example of measured dipole field distribution along an ideal curved axis. One can see that the magnetic field forms a smooth and step-wise distribution as expected, and the field strengths match the design values.

Figure 1: Permanent magnet based longitudinal gradient bending magnet. The total length is about 1.7 meter.
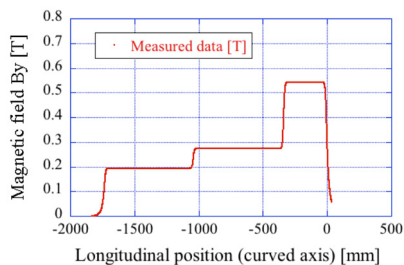
† twatanabe@spring8.or.jp

Figure 2: Measured magnetic field for the LGB in Fig.1.

All multipole magnets are laminated electromagnets. The bore diameters of quadrupole and sextupole magnets are respectively 34 and 36 mm. Although multipole electromagnets are rather conventional technologies, a compactness of coil winding, a physical repeatability of yokes, and precise engineering for µm-order alignments, etc. are considered in the design. After individual magnetic field measurements, the multipole magnets are aligned on a common girder as presented in Fig. 3. There are 3 common girders in the half-cell.
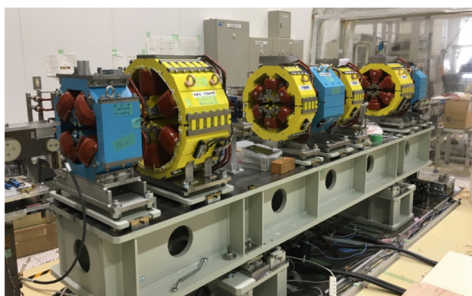

Figure 3: Quadrupole (blue) and sextupole (yellow) electromagnets on a common girder.

Magnet Alignment

Magnets have to be aligned along a designated path, especially for adjacent magnets. Our target is to align adjacent multipole magnets on a girder with the error of about ±10 µm, although there are some redundancies from beam dynamics. For the purpose, we have adopted the vibrating wire scheme [5] and investigated detailed performances [6]. The advantage is that one can align magnets while directly observing its magnetic center, but we have to verify effects of a wire sag and repeatability of measurement. Therefore, we first align all the multipole magnets on a girder. According to the wire measurement, it showed that all the magnets were aligned within 5 µm. Then we repeated the measurement by intentionally removing and resetting a wire. Figure 4 indicates an example of measured center positions for a given quadrupole magnet after adjusting the wire position at both end magnets each time. All the circles are found within ±5 µm. The result was obtained after removing residual vibration due to background fields.

Note, however, that the overall precision of the alignment cannot simply be measured by the result. For example, the effect of a wire sag is not included in Fig. 4, while in a practical alignment, one has to make sure that magnets are aligned not along a curved wire but in a straight line. Also, mechanical repeatability of magnet yokes after splitting the magnet affects the overall precision of alignment. The drift of magnet center is also of concern. These effects are being evaluated and summarized.
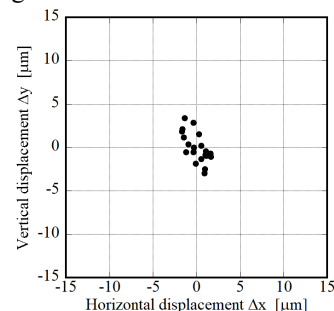

Figure 4: Quadrupole magnet center positions repeatedly measured by vibrating wire scheme.

VACUUM COMPONENTS

The increases in the number of magnets as well as photon absorbers, resulting from the multi-bend configuration, bring space constraints in a longitudinal axis. The decrease in bore diameters of magnets results in space constraints in transverse dimensions. In addition, one-year shutdown needs to be considered. Taking these constraints into consideration, we have developed new vacuum components and pumping strategies [7].

It then ends up with a 12-meter-long stainless steel vacuum chamber that covers almost a half-cell of the new lattice. The long integrated chamber only has two gate valves at both ends for saving space. The material of stainless steel helps avoid the physical interference with small-diameter magnets by its thinner cross section. It is also beneficial to remove transition chambers between stainless steel and other material parts. Thus the thinner chamber enables us to maintain ante structures, where vacuum pumping will be discretely provided by NEG cartridges and SIPs. We intend to implement the baking and the NEG activation before installing the vacuum chamber into the tunnel. It is expected to help shorten the installation procedure from the vacuum side.

Figure 5 presents a test 12-meter vacuum chamber. Between the two gate valves, two bending unit chambers and three straight unit chambers are connected with each other by welding. At the downstream end of the bending unit chamber, a photon absorber at the location of the end of bending magnet is inserted from the outside of the chamber for cutting synchrotron radiation emitted from an upstream bending magnet. At straight unit chambers, photon absorbers and crotch absorbers are attached from the upside of the chamber. In processing each unit chamber, most of parts are annealed at 900 °C for 10 minutes to keep the relative permeability below 1.05 after mechanical processing and laser beam welding. The annealing is also expected to reduce thermal desorption. Then each unit chamber will be assembled by TIG welding. Finally, the 12-meter chamber is assembled, baked at 150 °C, and NEG activated. In Fig. 5, the test 12-meter chamber is transported from the assembling room into the

actual accelerator tunnel for demonstrating the installation scenario. The chamber will be introduced to the test half-cell, and we will keep updating the vacuum component designs and the installation scenario.

Figure 5: 12-meter vacuum chamber for installation test.

RF COMPONENTS

RF cavities and most of other RF components will be reused for SPring-8-II. Due to the lower electron energy, the number of RF cavities will be reduced from 32 (present) to 16. The RF frequency will be slightly increased from 508.58 to 508.76 MHz due to a bit shorter circumference for SPring-8-II. We will preserve exiting four RF stations but rearrange high power RF configurations.

Looking for a future option, we have developed a new RF cavity based on TM020 mode with a compact slot-type HOM damper inside the cavity [8]. The damper slots are placed along the magnetic node of TM020 for absorbing harmful parasitic resonance modes. The new cavities are expected to be useful not only to SPring-8-II but also other light sources.

For low-level RF (LLRF) system, we have developed new digital system, introducing MTCA.4 based modules, EtherCAT field bus, and under-sampling RF detection [8]. In April 2018, the new LLRF was installed to one of the four RF station at SPring-8. After some debugs, the new system provides stable beam operations with the amplitude stability of less than 10^{-3}, and the phase stability of less than 0.05 degree. Thus, we will renew all the LLRF system prior to the SPring-8-II upgrade.

MONITORS

An accurate and stable beam position monitor (BPM) is one of key instrumentations to achieve smooth beam commissioning and stable beam operations [9]. The resolution for closed orbit distortions should be 0.1 μm rms or less at 1 kHz BW, 10 Hz repetition rate. That for single-pass trajectory should be 100 μm rms for a turn-by-turn measurement of injected beam. We have finished the test fabrication of the BPM head as schematically illustrated in Fig. 6. According to our evaluation, the error between mechanical and electrical centers should be within ±80 μm. The test BPM head has been installed to the current storage ring of SPring-8 with some modification for existing vacuum enclosures, with which we have been observing the stability and other specifications for a year. So far, we have obtained the COD-BPM resolution of about 10 nm rms (not shown here), and the stability of 1 μm/month

(Fig. 7). We will continue the date acquisition. The test BPM heads with dummy electrodes have been welded in the 12-meter vacuum chamber. We also have designed and developed readout electronics for the BPM system. The RF front-end circuit has already been manufactured, and is now being evaluated its performance.

Other instrumentations such as current transformers (CTs), screen monitors, and bunch-by-bunch feedback (BBF) system are as well being developed.
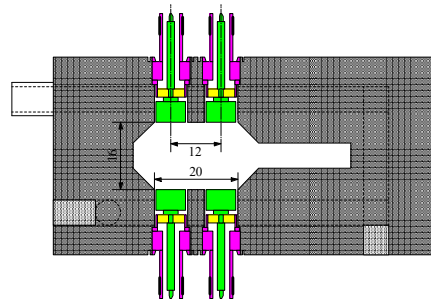

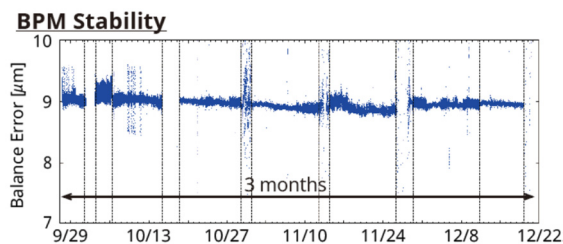Figure 6: Schematic view of BPM head.

Figure 7: COD-BPM test run at SPring-8.

SUMMARY

The SPring-8-II project aims at achieving a significant leap of light source performance with some considerations for stability, reliability, and energy consumption. In addition to detailed study of beam dynamics [2, 10], hardware developments have been extensively implemented and a number of positive results have been obtained. These works are expected to be beneficial not only to SPring-8-II but also to other accelerators such as a 3 GeV new light source possibility in Japan.

REFERENCES

[1] H. Tanaka *et al.*, in *Proc. 7th Int. Particle Accelerator Conf. (IPAC'16)*, Busan, Korea, May 2016, p. 2867.

[2] K. Soutome *et al.*, in *Proc. 7th Int. Particle Accelerator Conf. (IPAC'16)*, Busan, Korea, May 2016, p.3440.

[3] J. Chavanne *et al.*, in *Proc. 5th Int. Particle Accelerator Conf. (IPAC'14)*, Dresden, Germany, Jun. 2014, p. 968.

[4] T. Watanabe *et al.*, PRAB 20, 072401, 2017.

[5] A. Jain *et al.*, in *Proc. IWAA2008*, Tsukuba, Japan, 2008, TU010.

[6] K. Fukami *et al.*, in *Proc. IWAA16*, Grenoble, France. https://indico.cern.ch/event/489498/contributions/2217459/

[7] M. Oishi *et al.*, in *Proc. 7th Int. Particle Accelerator Conf. (IPAC'16)*, Busan, Korea, May 2016, p. 3651.

[8] H. Ego *et al.*, in *Proc. 7th Int. Particle Accelerator Conf. (IPAC'16)*, Busan, Korea, May 2016, p. 414.

[9] H. Maesaka *et al.*, in *Proc. 7th Int. Particle Accelerator Conf. (IPAC'16)*, May 2016, p. 149; and H. Maesaka *et al.*, in *Proc. 8th Int. Particle Accelerator Conf. (IPAC'17)*, Copenhagen, Denmark, May 2017, p. 265.

[10] K. Soutome and H. Tanaka, PRAB 20, 064001, 2017.